EFFECT OF MARTENSITE DISTRIBUTION ON STRAIN DISTRIBUTION AND UNIFORM ELONGATION IN DUAL-PHASE STEELS; COMPARISON BETWEEN A SEGREGATION NEUTRALISED GRADE AND A COMMERCIAL GRADE

[1]Pedram DASTUR, [1]Carl SLATER, [1]Claire DAVIS

[1]WMG, University of Warwick, Coventry, United Kingdom, pedram.dastur@warwick.ac.uk

https://doi.org/10.37904/metal.2024.4880

Abstract

Dual-phase steels, commonly employed in the automotive industry, are characterised by their ferrite and martensite microstructure. In many cases, the martensite can be seen to be banded in the rolling direction. This banded microstructure arises from micro-segregation during solidification, primarily of manganese followed by subsequent rolling. The martensite banding can degrade the uniform elongation and ductility. In this study, the concept of altering the morphology of martensite has been employed to enhance the uniform elongation of DP steel. In this context, the influence of manganese segregation on the distribution of the second phase has been neutralised by redesigning the steel composition compared to conventional DP grades. The new DP steel grade has been introduced as 'segregation-neutralised (SN)' DP steel. A combination of micromechanical finite element modelling and uniaxial tensile tests was utilised to study the effect of change in the distribution of martensite on strain distribution and uniform elongation in DP steel. The strain-field measurement from the finite element modelling revealed a more homogeneous shear band formation in SN-DP, resulting in a decrease in the frequency of the high-localised strain regions in SN-DP compared to a commercially benchmarked DP grade. Tensile results also showed an improvement in uniform elongation in SN-DP (+2.3 % absolute) compared to the benchmark DP grade with similar tensile strength.

Keywords: Dual-phase steel, martensite morphology, strain distribution, uniform elongation

1. INTRODUCTION

Dual-phase (DP) steels, classified as first-generation advanced high-strength steels (AHSS), are employed in the automotive industry due to their optimal balance of strength and ductility [1]. Given the increasing interest in reducing the weight of automobile parts, there is a continual effort to improve the mechanical properties of existing DP steel grades [2]. DP steels are distinguished by a microstructure comprising a softer ferrite phase and a banded configuration of the harder martensite phase [3]. This banding of martensite is largely attributed to the segregation of manganese (Mn) to inter-dendritic zones during the casting and subsequent rolling processes, resulting in banded regions with increased Mn content. As Mn is an austenite stabilising element, the Ac_1 temperature is decreased in the Mn-rich regions, which results in the preferred formation of austenite/martensite in these regions. Negative influences on the mechanical properties of DP steels due to the banded morphology of martensite have been documented. Tasan et al. [4] analysed the influence of martensite bands on strain localization in a DP steel using digital image correlation (DIC). They reported significant strain localisation near large, banded martensite, which caused local void formation and/or martensite cracking, leading to early failure during straining. Ramazani et al. [5] altered the banded martensite morphology to a non-banded form in their DP microstructure (35 % martensite fraction) by adjusting the heating rate and annealing temperature. This modification resulted in enhanced tensile strength and a 2 % improvement in uniform elongation in the DP microstructure with non-banded martensite. Matsuno et al. [6] investigated the effect of martensite banding using finite element (FE) modelling of 3D Voronoi DP microstructures (28 % martensite fraction). Their findings indicated that martensite banding reduced uniform

elongation by approximately 6% but significantly increased tensile strength by about 200 MPa, contrasting with the findings of Ramazani et al. [5]. A detailed comparison between the two studies highlighted differences in the martensite distribution within their non-banded microstructures. In this regard, the challenge of accurately representing martensite banding in two-dimensional analyses has been cited as a reason for the conflicting results observed in various studies.

Altering the morphology and distribution of martensite has been identified as a promising strategy for enhancing the mechanical properties of DP steels. Extensive research has been directed towards removing the banded distribution of martensite in these steels. These studies typically involve complex laboratory-based thermal cycles, either involving immediate quenching from the austenitisation temperature to room temperature [7] or employing multiple heating and cooling steps [8]. However, these methods are not practical in a steel manufacturing environment. To date, no studies have reported on DP steels processed using contemporary industrial methods that produce equiaxed and uniformly dispersed martensite, where both the morphology and distribution are altered from the conventional banded martensite microstructure. In our previous work [9], the concept of segregation-neutralised DP steel (referred to as "SN-DP") was introduced as a means to achieve a non-banded distribution of martensite using standard continuous annealing thermal cycles. The strategy involved adjusting the composition of conventional DP steel grades by modifying the ratio of manganese to silicon. This balance between the austenite-stabilising effect of manganese and the ferrite-stabilising effect of silicon minimises the difference in the Ac_1 temperature between solute-rich interdendritic regions and solute-poor dendritic regions. In the current study, a comparative analysis of the strain distribution and uniform elongation of SN-DP steel has been conducted relative to a benchmark banded martensite commercial composition DP (BM-DP) steel.

2. EXPERIMENTAL METHODS AND MICROMECHANICAL SIMULATION METHODOLOGY

The compositions of the steels used in this study are detailed in **Table 1**. The first composition shows the BM-DP composition and the second outlines the composition of SN-DP steel. The BM-DP steel produced in the laboratory was benchmarked against a commercial DP steel to ensure that it matched in terms of martensite distribution and mechanical properties [10]. The chemical basis for the SN-DP design has been discussed in our previous work [9]. Both steels were vacuum induction-melted (VIM) and cast into 10 kg ingots, followed by hot rolling and then cold rolling into steel sheets. Post-cold roll intercritical annealing was then carried out to achieve the final microstructures. Scanning electron microscopy (SEM) using a JEOL JSM-7800F system, equipped with electron backscattered diffraction (EBSD) from Oxford Instruments Symmetry S2, was employed to characterise the DP microstructures. Mechanical analysis of the samples was conducted through uniaxial tensile testing using a miniature sample size, with a gauge length of 10 mm, on an Instron 30 kN tensile machine. The tests were performed at a displacement rate of 0.4 mm/min. Micromechanical finite element method (FEM) simulations were employed to analyse the strain partitioning between ferrite and martensite in microstructures with varying distributions of the second phase. The representative volume element (RVE) used for these FEM simulations was derived from reclassified EBSD images of the experimental microstructures. The geometric meshing of RVEs and the solving of the FEM simulations were performed in COMSOL Multiphysics 6.2. For the boundary condition, a predefined displacement was applied to one edge of the RVE frame and symmetry conditions were imposed along the other two intersecting edges of the RVE frame. The flow stress behaviour was sourced from the literature [6,11]. Swift law was used for ferrite:

$$Y = C(\varepsilon_0 + \varepsilon_P)^n \quad (1)$$

Where: C = 760 MPa, ε_0 = 0.02 and n = 0.3. For martensite, Voce law was employed:

$$Y = Y_0 + (Y_{sat} - Y_0)(1 - exp^{(-C_Y \varepsilon_P)}) \quad (2)$$

Where: Y_0 = 1000 MPa, Y_{sat} = 2650 MPa and C_y = 70.

Table 1 Chemical compositions of DP steel grades used in this study (wt%)

DP steel grade	Fe	C	Mn	Si	Cr	Nb	B	Ti
BM-DP	Bal.	0.13	1.86	0.25	0.55	0.03	0.000	0.02
SN-DP	Bal.	0.13	0.25	0.75	0.55	0.03	0.003	0.015

3. RESULTS AND DISCUSSION

3.1. Microstructures

The phase-classified maps (obtained from EBSD analysis) of the heat-treated BM-DP and SN-DP are shown in **Figure 1a** and **Figure 1b**, respectively**.** Both microstructures are composed of only ferrite and martensite phases. The fraction of martensite in both microstructures is relatively similar, with values of 30.2 ± 0.5 % and 30.7 % ± 1.6 % in BM-DP and SN-DP, respectively. Furthermore, the ferrite grain size is almost the same in both microstructures. The area-weighted average grain size values are 10.35 µm ± 0.5 µm and 10.11 µm ± 0.4 µm in BM-DP and SN-DP, respectively. However, a clear difference in morphology and distribution of martensite can be observed between the two microstructures. A banded morphology of martensite can be observed in the microstructure of BM-DP, while in SN-DP, the martensite islands are distributed as separate, discrete regions with no banding observed. The morphology and distribution of martensite were quantified for better comparison between the two grades. The average value of martensite particle size was used to assess the distribution of martensite between the two phases (**Figure 1c)**. As the volume fraction of martensite in both microstructures is almost identical, the average martensite size is representative of martensite distribution. To compare the morphology of martensite, the average aspect ratio of martensite was employed (**Figure 1c)**. For each index, a significant distinction can be observed between the two microstructures. The higher value of the average martensite size in BM-DP indicates that the connectivity of the martensite is higher in BM-DP compared to SN-DP microstructure. The aspect ratio of the martensite in the BM-DP microstructure is almost three times higher than that in the SN-DP microstructure. This is related to the more equiaxed martensite shapes in SN-DP compared to BM-DP.

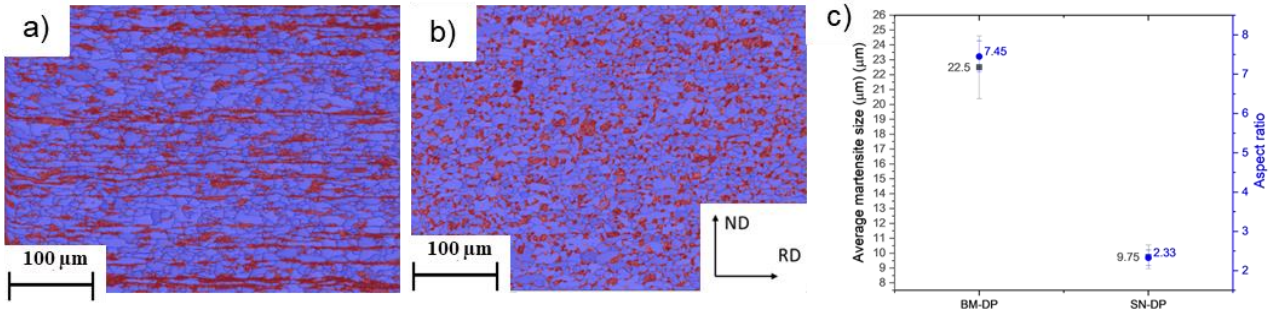

Figure 1 a) and b) phase-classified maps of the heat-treated BM-DP and SN-DP c) average martensite size and average aspect ratio in BM-DP and SN-DP

3.2. Strain distribution

Figure 2a and **Figure 2d** illustrate the generated RVEs used for BM-DP and SN-DP for micromechanical FEM simulation. These RVEs were obtained from the corresponding phase-classified maps. The microstrain distribution maps from the FEM simulation are shown in **Figure 2b** and **Figure 2e** for the engineering strain of 19.5 %. The formation of shear bands can be observed in both RVEs, with an average angle of 45 degrees. The number and homogeneity of shear bands differ between BM-DP and SN-DP RVEs. In BM-DP, with higher connectivity of martensite, fewer but stronger shear bands can be observed compared to SN-DP, which are

localised in specific parts of the microstructure. The presence of martensite bands acts as a barrier to slip deformation in ferrite, leading to shear bands preferentially forming between martensite bands. Conversely, in SN-DP, due to the lower connectivity of martensite, there are more spaces between martensite islands through which shear bands can pass.

The strain distribution curves (fitted normal distribution) in ferrite and martensite at the engineering strain of 19.5 % are shown in **Figure 2c** and **Figure 2f**, respectively. A shift in the distribution of equivalent plastic strain in martensite towards higher strain values can be observed in BM-DP compared to SN-DP. The average plastic strain of martensite in BM-DP (~8 %) was almost 4 % higher compared to SN-DP (~4 %). On the other hand, the peak of the strain distribution curve in the ferrite phase is higher in SN-DP than in BM-DP, indicating that ferrite in SN-DP (average plastic strain = 29 %) has experienced greater average plastic deformation compared to BM-DP (average plastic strain = 27 %). However, the tail end of the strain distribution curve in BM-DP is even slightly higher than SN-DP. The observation of a higher frequency of high-strain regions in the BM-DP, particularly within the martensite phase, indicates that the rate of void formation is likely greater in BM-DP compared to SN-DP.

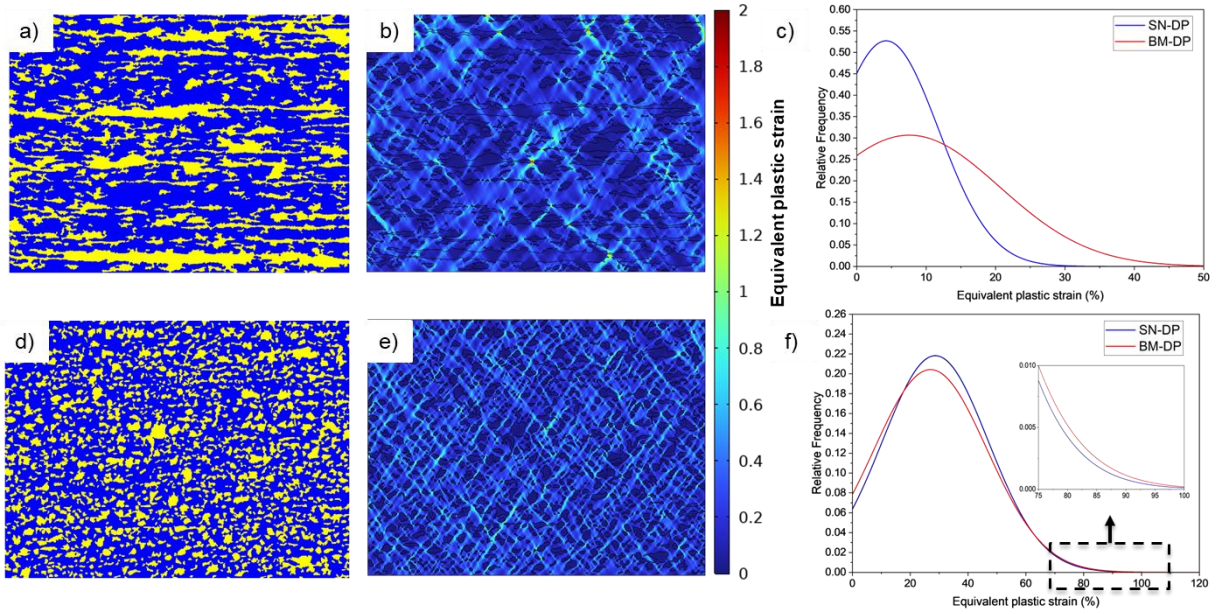

Figure 2 a) and d) RVEs used for FE simulation in BM-DP and SN-DP, respectively, b) and e) local equivalent plastic strain maps in BM-DP and SN-DP, respectively, c) and f) histograms of local strain distribution in martensite and ferrite, respectively at the engineering strain of 19.5%

3.3. Tensile properties

The engineering stress-strain curves of the heat-treated BM-DP and SN-DP are shown in **Figure 3a**. In both tensile curves a continuous yielding is observed, which indicates the existence of mobile dislocations at the ferrite/martensite interface. In DP steel grades, as a result of austenite to martensite transformation, these mobile dislocations are generated at the ferrite/martensite interface [12,13]. The average values of ultimate tensile strength (UTS), uniform elongation and total elongation for each DP grade are given in **Table 2.** Given the considerable disparity in the post-uniform elongation values observed between specimens, the associated error bar for total elongation was relatively high. Consequently, only uniform elongation values are considered for comparison between the two grades. Regarding tensile strength, both grades exhibited an almost similar UTS value (~760 MPa), while the uniform elongation was improved by approximately 2.3% in SN-DP compared to BM-DP. According to the strain hardening curves (**Figure 3b**), the strain hardening rate in BM-DP is higher

compared to SN-DP at the initial stage of plastic deformation. However, after a specific tensile strain, the rate of decline in the strain-hardening rate is faster in BM-DP compared to SN-DP, resulting in a lower uniform elongation. The difference in strain hardening behaviour between the two grades can be explained by the higher plastic deformation of martensite in the BM-DP microstructure (**Figure 2c**). The higher initial strain hardening rate in BM-DP can be attributed to the higher initial strain hardening rate of the martensite phase compared to the ferrite phase [14]. However, the strain hardening rate of martensite approaches zero after reaching a specific plastic strain known as saturation point. Furthermore, if the martensite phase undergoes higher plastic deformation, a higher void formation rate is expected, which facilitates the strength-weakening phenomenon during plastic deformation [15]. Consequently, the strain hardening rate dropped at lower plastic strains in BM-DP compared to SN-DP. The lower uniform elongation observed in the banded microstructure (BM-DP) is consistent with the findings of Matsuno et al. [6] and Ramazani et al. [5], where higher uniform elongation was observed in the DP microstructures with equiaxed martensite.

A diagram of tensile strength-uniform elongation was plotted in **Figure 3c** to facilitate a comparison of the strength-elongation balance between BM-DP and SN-DP. In addition, a few more data points based on samples with different fractions of martensite and the hot-rolled samples have been included in this diagram. An allometric curve was then fitted on the data points for each DP grade. The fitted curve has shifted to a more upright position in the strength-elongation diagram indicating an enhanced combination of strength and uniform elongation in SN-DP compared to BM-DP samples.

Table 2 Tensile properties of the heat-treated BM-DP and SN-DP

DP steel grade	UTS (MPa)	Uniform elongation (%)	Total elongation (%)
BM-DP	761 ± 8	11.8 ± 0.5	16.1 ± 4.1
SN-DP	768 ± 15	14.1 ± 0.6	18.5 ± 3.8

4. CONCLUSION

The concept of segregation-neutralised DP steel was used to change the banded morphology of martensite in a conventional DP grade to an equiaxed and well-dispersed distribution. The strain distribution maps from FEM results revealed that there are fewer but stronger shear bands in the BM-DP microstructure compared to SN-DP. Based on FEM results, BM-DP showed almost 4 % absolute higher average plastic deformation in martensite during straining compared to SN-DP. Although the average plastic strain in ferrite was lower in BM-DP, the frequency of high-strain regions in ferrite was slightly higher in BM-DP. The tensile results indicated that at a comparable tensile strength (~760 MPa), uniform elongation was improved from 11.8 % in BM-DP to 14.1 % in SN-DP.

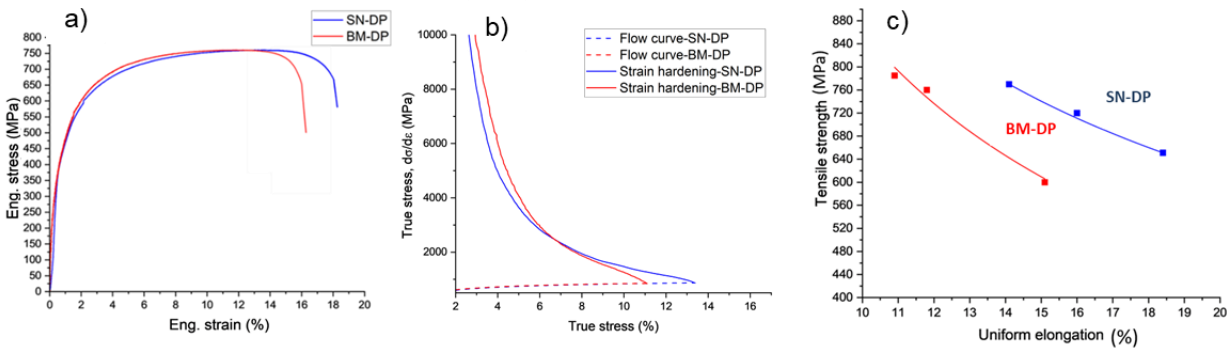

Figure 3 a) Engineering stress-strain curves, b) strain-hardening and true stress-strain curves of BM-DP and SN-DP, c) diagram of tensile strength-uniform elongation comparing BM-DP and SN-DP samples.

REFERENCES

[1] TASAN, C.C., DIEHL, M., YAN, D., BECHTOLD, M., ROTERS, F., SCHEMMANN, L., ZHENG, C., PERANIO, N., PONGE, D., KOYAMA, M., TSUZAKI, K., RAABE, D. An Overview of Dual-Phase Steels: Advances in Microstructure-Oriented Processing and Micromechanically Guided Design. Annual Review of Materials Research. 2015, vol. 45, pp. 391-431. https://doi.org/10.1146/annurev-matsci-070214-021103.

[2] KEELER, S., KIMCHI, M., MOONEY, P.J. Advanced High-Strength Steels Guidelines Version 6.0. WorldAutoSteel. 2017, p. 314. https://www.worldautosteel.org/projects/advanced-high-strength-steel-application-guidelines/.

[3] KREBS, B., GERMAIN, L., GOUNÉ, M., HAZOTTE, A. Banded structures in dual-phase steels - A novel characterization method. International Journal of Materials Research. 2011, vol. 102, pp. 200-207. https://doi.org/10.3139/146.110467.

[4] TASAN, C.C., HOEFNAGELS, J.P.M., GEERS, M.G.D. Microstructural banding effects clarified through micrographic digital image correlation. Scripta Materialia. 2010, vol. 62, pp. 835-838. https://doi.org/10.1016/j.scriptamat.2010.02.014.

[5] RAMAZANI, A., MUKHERJEE, K., PRAHL, U., BLECK, W. Modelling the effect of microstructural banding on the flow curve behavior of dual-phase (DP) steels. Computational Materials Science. 2012, vol. 52, pp. 46-54. https://doi.org/10.1016/j.commatsci.2011.05.041.

[6] MATSUNO, T., YOSHIOKA, T., WATANABE, I., ALVES, L. Three-dimensional finite element analysis of representative volume elements for characterizing the effects of martensite elongation and banding on tensile strength of ferrite-martensite dual-phase steels. International Journal of Mechanical Sciences. 2019, vol. 163, p.105133. https://doi.org/10.1016/j.ijmecsci.2019.105133.

[7] SHAHZAD, M., TAYYABA, Q., MANZOOR, T., UD-DIN, R., SUBHANI, T., QURESHI, A.H. The effects of martensite morphology on mechanical properties, corrosion behavior and hydrogen assisted cracking in A516 grade steel. Materials Research Express. 2018, vol. 5, p.016516.

[8] SRIVASTAVA, A.K., PATEL, N.K., RAVI KUMAR, B., SHARMA, A., AHN, B. Strength–Ductility Trade-Off in Dual-Phase Steel Tailored via Controlled Phase Transformation. Journal of Materials Engineering and Performance. 2020, vol. 29, pp. 2783-2791. https://doi.org/10.1007/s11665-020-04799-6.

[9] SLATER, C., BANDI, B., DASTUR, P., DAVIS, C. Segregation Neutralised Steels: Microstructural Banding Elimination from Dual-Phase Steel Through Alloy Design Accounting for Inherent Segregation. Metallurgical and Materials Transactions A: Physical Metallurgy and Materials Science. 2022, vol. 53, pp. 2286-2299. https://doi.org/10.1007/s11661-022-06674-6.

[10] ZHU, Y., SLATER, C., CONNOLLY, S., FARRUGIA, D., DAVIS, C. Rapid alloy prototyping for strip steel development: DP800 steel case study. Ironmaking and Steelmaking. 2021, vol. 48, pp. 1-12. https://doi.org/10.1080/03019233.2021.1880036.

[11] MATSUNO, T., TEODOSIU, C., MAEDA, D., UENISHI, A. Mesoscale simulation of the early evolution of ductile fracture in dual-phase steels. International Journal of Plasticity. 2015, vol. 74, pp. 17-34. https://doi.org/10.1016/j.ijplas.2015.06.004.

[12] ZHAO, Z., TONG, T., LIANG, J., YIN, H., ZHAO, A., TANG, D. Microstructure, mechanical properties and fracture behavior of ultra-high strength dual-phase steel. Materials Science and Engineering A. 2014, vol. 618, pp. 182-188. https://doi.org/10.1016/j.msea.2014.09.005.

[13] AVENDAÑO-RODRÍGUEZ, D., GRANADOS, J.D., ESPEJO-MORA, E., MUJICA-RONCERY, L., RODRÍGUEZ-BARACALDO, R. Fracture mechanisms in dual-phase steel: Influence of martensite volume fraction and ferrite grain size. Journal of Engineering Science and Technology Review. 2018, vol. 11, pp. 174-181. https://doi.org/10.25103/jestr.116.22.

[14] PIERMAN, A.-P., BOUAZIZ, O., PARDOEN, T., JACQUES, P.J., BRASSART, L. The influence of microstructure and composition on the plastic behaviour of dual-phase steels. Acta Materialia. 2014, vol. 73, pp. 298-311. https://doi.org/10.1016/j.actamat.2014.04.015.

[15] XUE, L. Damage accumulation and fracture initiation in uncracked ductile solids subject to triaxial loading. International Journal of Solids and Structures. 2007, vol. 44, pp. 5163-5181. https://doi.org/10.1016/j.ijsolstr.2006.12.026.